

Nation Cheng Kung University
Institute of Space and Plasma Sciences
112 Annual Report

專題生：畢永葳

指導教授：張博宇

Data: 2024/02/05

Abstract

This report summarizes the activities carried out from 2023 to February 5, 2024. The main focus was on the design of the Tokamak device, involving the use of COMSOL to simulate the ohmic heating and cooling requirements of the coils. Benchmark calculations were performed to confirm the accuracy of the COMSOL simulations. Based on the simulation results, it was found that when the cross-sectional area of the coil was $20 \times 20 \text{ mm}^2$ and a driving current of 25 kA last for 500 ms, the coil temperature rised by approximately 10°C . No additional cooling is needed. Therefore, a cooling system will not be considered in the subsequent design of the Tokamak device. Additionally, we have developed an algorithm to calculate the eddy current in the inner vacuum vessel wall generated by the time-varying current of the central solenoid. Therefore, eddy currents generated within the Tokamak device can be computed so that more precise designs in subsequent Tokamak devices can be obtained. In addition, the eddy current will be included for calculating the breakdown voltage required for plasma generation and for determining the current of the central solenoid for inducing the plasma current. In conclusion, this report includes calculations for the ohmic heating and cooling system, as well as the eddy current calculation method applied in the Tokamak device.

Contents

1. Tokamak	4
2. Calculation of the ohmic heating of coils in Tokamak.....	5
2.1. Calculating the ohmic heating theoretically	5
2.2. Calculating the ohmic heating via COMSOL simulation.....	6
2.3. Conclusion	8
3. Confirming the accuracy of COMSOL heat transfer model	9
4. Calculation of the eddy current in the inner vacuum vessel wall generated by the time-varying current of the central solenoid.....	12
4.1. Selecting the central solenoid and inner vacuum vessel as the calculation targets	12
4.2. Using COMSOL to calculate inductance and resistance.....	13
4.3. Confirm the accuracy of COMSOL in calculating resistance and inductance.....	16
4.4. Calculation of the eddy current using the full circuit equation.....	21
4.5. Discussion.....	25
5. Future work.....	26
6. Conclusion	26
Reference	27

1. Tokamak

A Tokamak is a device used to achieve nuclear fusion through magnetic-confinement fusion (MCF). In our Tokamak device, we utilize magnetic fields produced by coils to generate plasma, drive plasma current, and confine the plasma. Consequently, in the design of Tokamak devices, it is crucial to accurately calculate the ohmic heating and cooling requirements of the coils to ensure stable operation within their load range. According to Ohm's law, when current flows through a conductor, heat is generated due to the presence of resistance, resulting from collisions between electrons and conductor atoms. It is known as ohmic heating. This affects the design of coils and cooling systems because cooling systems need to handle the heat generated by the ohmic heating, effectively dissipating heat to prevent coil from being overheated. Additionally, cooling systems must also maintain the coil material at an appropriate temperature to preserve coil from expanding. Thus, we can ensure the stability and the durability of the device. Furthermore, during device operation, the time-varying current in the coil generates magnetic field, inducing eddy currents in other coils and structures, which lead to deviations in calculated magnetic fields. The electromagnetic forces act on the structures due to the eddy currents also need to be considered. Therefore, before constructing Tokamak devices, it is necessary to calculate the induced currents generated within the device and incorporate them into design calculations to obtain more accurate results.

This report consists of five sections: (1) Calculation of the ohmic heating of coils in Tokamak; (2) Confirm the accuracy of COMSOL heat transfer model; (3) Calculation of the eddy current in the inner vacuum vessel wall generated by the time-varying current of the central solenoid; (4) Future work; and (5) Conclusion.

2. Calculation of the ohmic heating of coils in Tokamak

This section consists of three subsections: (1) Confirm the design of the central column of the toroidal magnetic field coil and confirm that additional cooling water cooling is not required; (2) Confirm the accuracy of COMSOL simulation for ohmic heating; and (3) Conclusion.

2.1. Calculating the ohmic heating theoretically

Before designing the cooling requirements for the coils, we first need to calculate the temperature rise caused by ohmic heating due to the current flow and determine whether cooling water is necessary or not.

The specifications of our Tokamak are as follows: at $R = 0.48$ m, the maximum toroidal magnetic field $B_T = 0.5$ T. In other words, the current required at the center is:

$$N \cdot I = \frac{2\pi RB}{\mu_0} = 1.2 \times 10^6 \text{ A} - \text{turn}, \quad (1)$$

assuming there is no cooling system, the energy generated by ohmic heating when the current passes through the coil will increase the coil temperature. Through a simple heat balance, we can obtain the temperature rise ΔT on the coil as:

$$R \int I^2 dt = m C_p \nabla T \Rightarrow \eta \frac{L}{A} \int I^2 dt = \rho A L C_p \Delta T, \quad (2)$$

$$\Rightarrow \nabla T = \frac{\eta}{\rho A^2 C_p} \int I^2 dt \approx \frac{\eta I^2 \Delta t}{\rho A^2 C_p} \quad (3)$$

where R is the coil resistance, I is the current, m is the coil mass, C_p is the specific heat of the material, η is the resistivity, L and A are the length and cross-sectional area of the coil, respectively, ρ is the density of the wire, and Δt is the duration of the current. Without coil cooling, the temperature rise of the coil is not a function of the coil length L . We intend to use copper, which has the lowest resistivity and the highest thermal conductivity ($\eta = 1.68 \times 10^{-8} \Omega - \text{m}$, $\rho = 8960 \text{ kg}/\text{m}^3$,

$C_p = 385 \text{ J/kg}$). We plan to use a toroidal field coil consisting of 12 turns, with each turn comprising 4 loops, resulting in a total of 48 turns of the toroidal field coil. Therefore, the current is 25 kA. We choose a copper strip with a cross-sectional area of $20 \times 20 \text{ mm}^2$ and assume driving currents last for 100 ms (10 Hz) and 500 ms (2 Hz), respectively. Under conditions where the effect of skin depth is neglected (skin depths are 20.6 mm and 46.1 mm for 10 Hz and 2 Hz, respectively), the calculated results are shown in Table 1. The estimated temperature rise on the coil is approximately 10°C for a current last for 500 ms. Therefore, additional cooling is not required.

Table 1: Estimated results of temperature rise on toroidal coil.

N	$I(\text{kA})$	$A(\text{mm}^2)$	$\Delta t(\text{ms})$	$\Delta T(^{\circ}\text{C})$
48	25	20×20	100	1.9
48	25	20×20	500	9.5

2.2. Calculating the ohmic heating via COMSOL simulation

The theory presented in the previous section can only be used to calculate under simple conditions. Considering other factors such as different shapes, temperature non-uniformity, water cooling, etc., the simple theory can only provide us with estimation in orders of magnitude and cannot assist in detailed design. Therefore, we still need to perform simulations to aid in the final engineering design. Hence, it is necessary to conduct benchmark tests for the simulation software to be used in the future. We are using COMSOL to simulate phenomena such as coil heating, electromagnetic fields, electromagnetic forces, mechanical stresses, etc., in our system. In this stage, we will focus on benchmark testing for Ohmic heating.

We used the "Time-dependent" "Electromagnetic Heating" module in COMSOL to simulate the heating of copper wire. As shown in Figure 1-1(a), the copper wire is 100 mm long, 20 mm wide, and 20 mm high, with material parameters listed in

Table 2. A current of $I = 25 \text{ kA}$ flows through the copper wire along the direction with a length of 100 mm . We simulated the temperature of the copper wire at 100 ms and 500 ms , and the results are shown in Figure 1-1(b). At 100 ms and 500 ms , the temperatures of the copper wire are 26.9°C and 34.5°C , respectively, indicating temperature increases of 1.9°C and 9.5°C , which match the theoretical calculations in Table 1.

Through benchmark test comparing theory with COMSOL simulations, we confirmed the reliability of the COMSOL simulation. In the future, we will further test whether COMSOL simulations matches theoretical calculations when there is cooling water in the copper tube. If they match, we can use COMSOL to simulate our design and confirm whether our coil design will have overheating issues or not.

Table 2: Material Parameters for Copper Wire

Parameter	Value
Electrical conductivity	$5.9524 \times 10^7 \text{ (S/m)}$
Heat capacity @ constant pressure	385 J/(kg-K)
Relative permittivity	1
Density	8960 kg/m^3
Thermal conductivity	400 W/(m.K)
Reference impedance	0.006Ω
Initial temperature	25°C

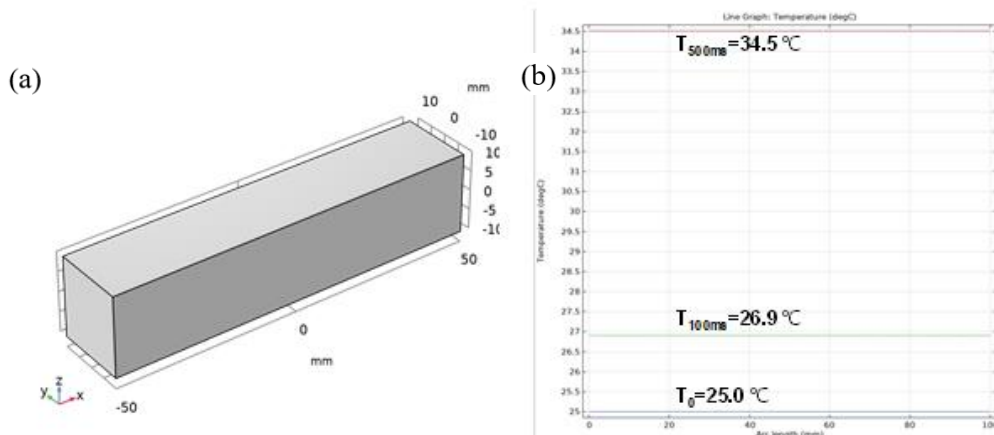


Figure 1-1: (a) Simulated Coil (b) Temperature at Initial, 100ms, and 500ms for Copper Wire

2.3. Conclusion

Through the calculations, we have confirmed that the temperature rise on our toroidal field coil is approximately 10°C for a duration of 500 ms, and we have confirmed that there is no requirement for additional cooling. Additionally, we have verified the reliability of the COMSOL simulation in the "Electromagnetic Heating" module. Therefore, we can utilize COMSOL to simulate detailed designs or complicated conditions in the future.

3. Confirming the accuracy of COMSOL heat transfer model

The purpose of this section is to verify the heating and cooling conditions of poloidal field coil and the central solenoidal. We plan to use water cooling inside copper pipes. It is essential to first confirm the accuracy of the heat transfer model in COMSOL.

Figure 2-1(a) depicts a cross-sectional view of the simulated copper pipe, which has an outer diameter of 11.28 mm. The hollow portion at the center with a diameter of 4 mm is filled with water. The initial temperature of both the copper pipe and water is set to 20°C. To validate the heat transfer model, we initially assume that the water is stationary and simulate the heating phenomenon of the copper pipe and water when a DC current of 2 kA flows through the copper pipe. Figure 2-1(b) shows the simulated results, with different curves representing temperature distributions at different times.

Since the temperature rise was not significant, we simulated a total time of 1 second. Initially, the input energy comes from the ohmic heating generated by the current passing through the copper pipe. The thermal conductivity of copper is much higher than that of water, resulting in almost uniform temperature distribution in the copper pipe. The distribution of water temperature is higher at the points where it contacts the copper pipe, and the central water temperature gradually increases over time. The distribution of curves aligns with qualitative analysis.

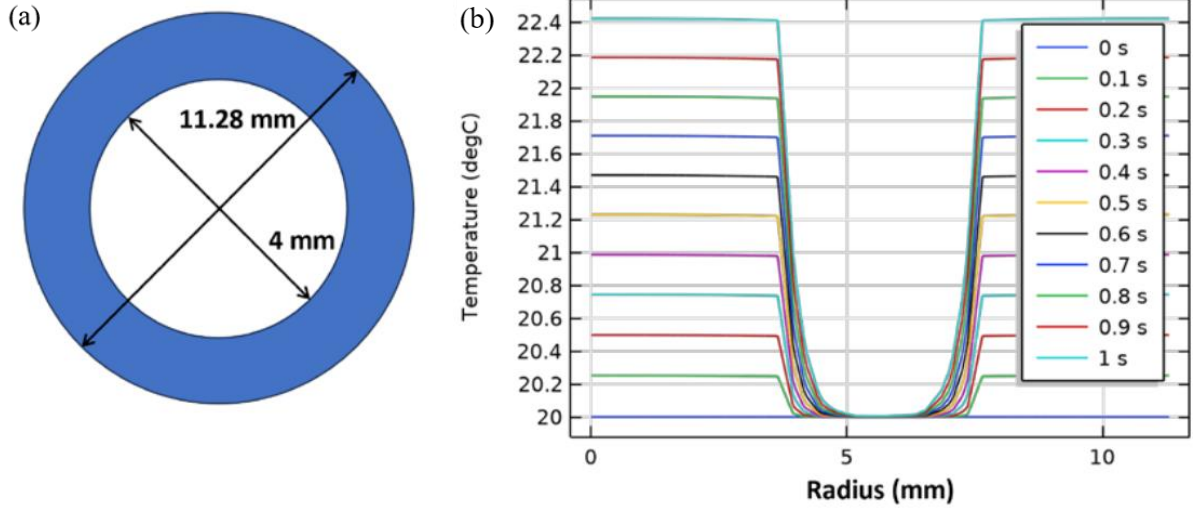


Figure 2-1: (a) Cross-sectional view of the copper pipe; (b) Temperature variation of the copper pipe and water along the red tangent line in Figure (a) over time.

We further verify if energy conservation is maintained in the simulation:

$$\int_0^t I^2 \eta \frac{L}{A_c} dt' = m_c C_p \Delta T_c + m_w C_w \Delta T_w, \quad (4)$$

$$I^2 \eta \frac{t}{A_c} = \rho_c C_p \int_{r_{c,min}}^{r_{c,max}} \Delta T_c(r) 2\pi r dr + \rho_w C_w \int_{r_{w,min}}^{r_{w,max}} \Delta T_w(r) 2\pi r dr \quad (5)$$

where the direct current $I = 2$ kA, η is the resistivity of copper, A_c is the cross-sectional area of copper, ρ_c and ρ_w are the densities of copper and water, respectively, C_p and C_w are the specific heats of copper and water, respectively, $\Delta T_c(r)$ and $\Delta T_w(r)$ are the temperature rises of copper and water at different radii r at time t , $r_{c,min} = 2$ mm, $r_{c,max} = 5.64$ mm, $r_{w,min} = 0$ mm, $r_{w,max} = 2$ mm. The 1st term in Eq.(4) is the ohmic heating generated in the conductor due to the current within the specified time interval. The 2nd and the 3rd term in Eq.(4) are the total heat absorbed by the copper pipe and water, respectively, calculated from their temperature change over time t .

At $t = 200$ ms the energy of ohmic heating is 153.835 J/m. According to the curve in Figure 5(b), the heating energy of the copper pipe is 149.559 J/m, and the heating energy of the water is 4.343 J/m. In other words, the total heating energy is

152.902 J/m, which is 0.6% different from the energy of ohmic heating. The discrepancy may come from the insufficient mesh refinement. Therefore, the heat transfer simulation in COMSOL is consistent with energy conservation.

As mentioned in subsection 2.1, when the cross-sectional area of the coil is $20 \times 20 \text{ mm}^2$, and a driving current of 25 kA last for 500 ms, the coil temperature rises by only 10°C , indicating no need for additional cooling. Therefore, the cooling system in the subsequent design of the device will no longer be considered.

4. Calculation of the eddy current in the inner vacuum vessel wall generated by the time-varying current of the central solenoid

In the Tokamak device, we will generate plasma, drive plasma current, and control plasma shape by adjusting the time-varying currents in coils such as poloidal field coil (PFC), toroidal field coil (TFC), and central solenoid (CS). However, the time-varying magnetic fields generated by these coils induce eddy currents in other coils and the vessel, which can negatively impact the originally calculated magnetic fields. Therefore, before constructing the Tokamak device, it is necessary to include the induced currents generated within the device into the design calculations to obtain more accurate results.

This section consists of five subsections: (1) Selecting the central solenoid and inner vacuum vessel as the calculation targets; (2) Using COMSOL to calculate inductance and resistance; (3) Confirm the accuracy of COMSOL in calculating resistance and inductance; (4) Calculation of the eddy current using the full circuit equation; and (5) Discussion.

4.1. Selecting the central solenoid and inner vacuum vessel as the calculation targets

Our device primarily relies on the time-varying current in the central solenoid (grey arrow in Figure 4-1) for plasma generation and driving plasma currents (orange arrow in Figure 4-1). Since the central solenoid is closed to the inner vacuum vessel wall, the wall is strongly affected by the changes of the magnetic field generated by the central solenoid. Therefore, this calculation focuses on computing the induced currents on the wall inside the vacuum vessel (indicated by the blue arrow in Figure 4-1) generated by the time-varying current in the central solenoid.

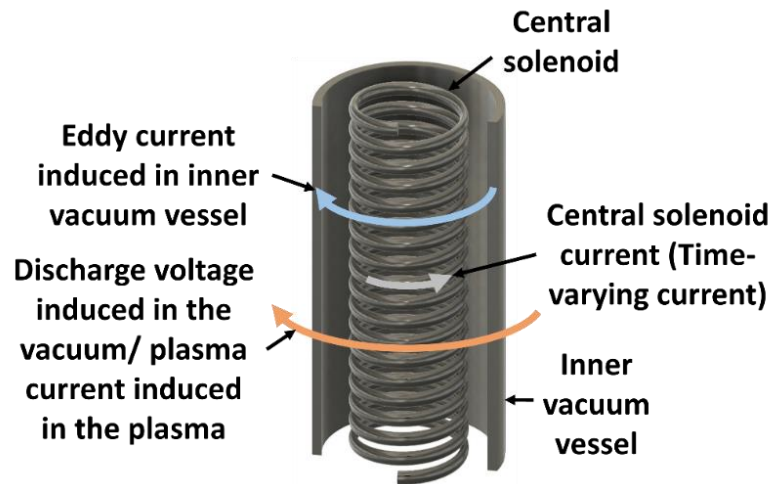


Figure 4-1: Schematic Diagram of Currents

4.2. Using COMSOL to calculate inductance and resistance

Before calculating the induced currents, we first need to compute the self-inductance, resistance, and mutual inductance between the central solenoid and the wall of the inner vacuum vessel. This can be done by utilizing the "Time-dependent" module of COMSOL's "Magnetic Fields" feature and conducting simulations of the magnetic field distribution in "2D Axisymmetric" mode.

The process of running the COMSOL simulation is the following:

- (1) In COMSOL, draw the cross-section of the central solenoid. Each turn of the central solenoid is a rectangular with a cross-sectional area of $11 \times 11 \text{ mm}^2$ with a hollow circle with a diameter of 4 mm at the center. The central solenoid is a double-layer coil with 115 turns in each layer, i.e. 230 turns in total. Then, depict the inner vacuum vessel wall, which is a cylinder with a length of 1600 mm, 150 mm in inner radius, and 4 mm in thickness, as shown in Figure 4-2(a).

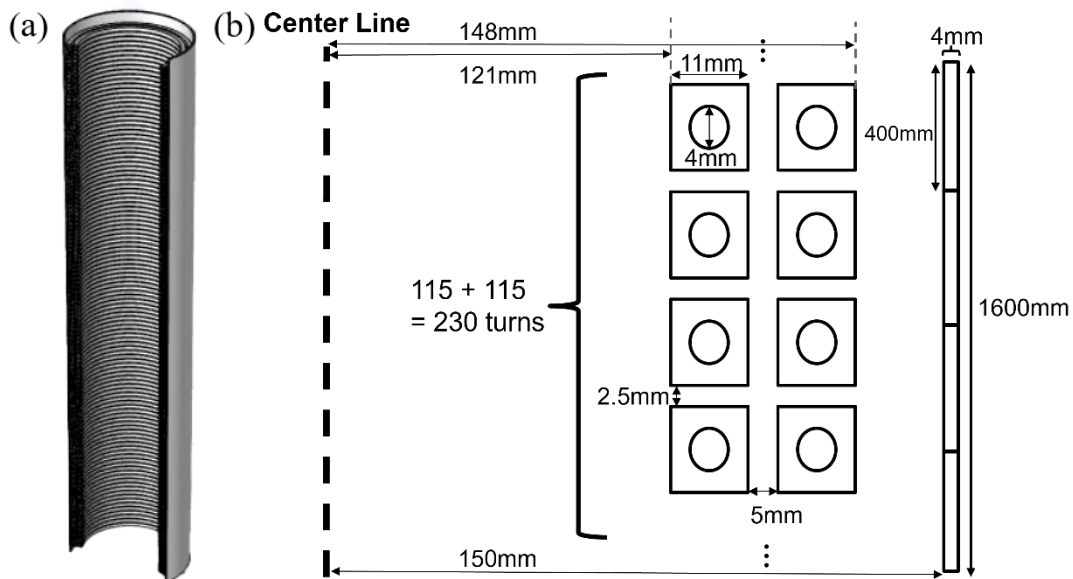


Figure 4-2(a): 3D Schematic Diagram of the Coil
 (b): 2D Schematic Diagram of the Coil Positions

(2) The boundary condition settings in simulation are crucial, as they can significantly impact the results. Therefore, within the "Layers" of the semi-circle set as the simulation domain, add an outer shell layer with a thickness of 50 mm.

(3) In the "Infinite Element Domain" option and in the right-click menu of "Definitions," select the previously drawn shell layer, as illustrated in Figure 4-3. This step ensures that the simulation boundary is not affected by the size of the semi-circle, thus ensuring the accuracy of the simulation.

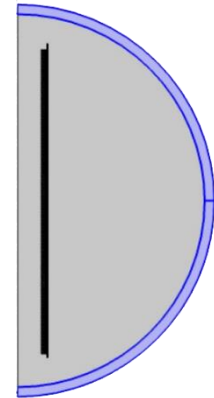


Figure 4-3:

(4) In the "Magnetic Fields" module, set central Infinite Boundary diagram solenoid and inner vacuum vessel wall as two separate "Coils". It is important to note that for the sake of convenience in drawing and simulation, we use "2D Axisymmetric" for simulation. We draw 230 square hollow coils to represent the central solenoid as shown in the figure. Therefore, when setting up the "Coil" for the central solenoid, make sure to check "Coil group" to treat all coils connected in series; otherwise, COMSOL will treat them as

connected in parallel.

(5) Set up two "Time-dependent" studies. During the simulation, COMSOL will automatically calculate their respective self-inductance, resistance, and mutual inductance:

(5a) "Study 1" simulates the magnetic field distribution when 1 A of current passes through central solenoid and 0 A of current passes through inner vacuum vessel wall.

(5b) "Study 2" simulates the magnetic field distribution when 0 A of current passes through central solenoid and 1 A of current passes through inner vacuum vessel wall.

(6) In "Global Evaluation", under "Results" in the right-click menu of "Derived Values", by entering the desired data names in the "Expression" field, we can export the calculated inductance and resistance.

(6a) In "Study 1," which simulates 1 A of current passing through the central solenoid with no current flowing through surrounding coils, we can obtain the resistance of the central solenoid, the self-inductance of the central solenoid, and the mutual inductance between central solenoid and the inner vacuum vessel wall. The corresponding data names in COMSOL are "mf.RCoil_1," "mf.LCoil_1," and "mf.L_2_1" respectively.

(6b) In "Study 2," we can calculate the resistance of inner vacuum vessel wall, the self-inductance of the walls, and the mutual inductance between the walls and the central solenoid. The corresponding data names in COMSOL are "mf.RCoil_2," "mf.LCoil_2," and "mf.L_1_2" respectively.

In the data names, "mf" stands for "Magnetic Fields" because the data we need to

export is calculated simultaneously with the simulation of magnetic fields. "RCoil" represents the coil's resistance, "LCoil" represents the coil's self-inductance, and "L_2_1" represents the mutual inductance between "Coil 1" (central solenoid), which generates magnetic flux passing through the surrounding coil "Coil 2" (inner vacuum vessel wall). Meanwhile, "L_1_2" represents the mutual inductance between "Coil 2" (the inner vacuum vessel wall), which generates magnetic flux passing through the surrounding coil "Coil 1" (central solenoid). The coil numbers "1" and "2" are automatically assigned by COMSOL when adding coils, but they can be edited in the "Coil name" setting of each coil. By following this approach, when the number of coils to be calculated increases, simply increase the number of "Coils" and "Studies," and the required data can be calculated accordingly using names like "mf.RCoil_3," "mf.LCoil_3," "L_3_1," and so on.

4.3. Confirm the accuracy of COMSOL in calculating resistance and inductance

Before proceeding with subsequent calculations using the inductance and resistance computed in COMSOL, we first need to confirm the accuracy of the COMSOL calculations.

To do this, we start by computing a simple model for benchmark. First, we used two co-center, parallel single-loop coils with different radius in COMSOL:

- (1) Draw two single-loop, coils with radii $R_1 = 100$ mm and $R_2 = 10$ mm, both with a radius $r_0 = 1$ mm, made of copper material, as shown in Figure 4-4.
- (2) Set the "Coil name" of the outer coil to "1" and the "Coil name" of the inner coil to "2".
- (3) Set up two "Time-dependent" studies:
 - (3a) "Study 1" simulates the magnetic field distribution when 1 A of current passes through "Coil 1" and 0 A of current passes through "Coil 2".

(3b) "Study 2" simulates the magnetic field distribution when 0 A of current passes through "Coil 1" and 1 A of current passes through "Coil 2".

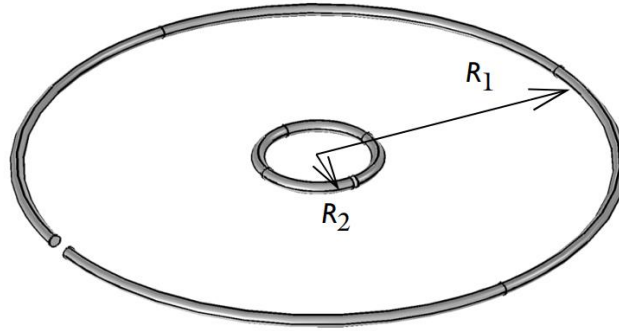


Figure 4-4: Coil Schematic Diagram

The simulation results are shown in Table 3.

Table 3: Simulation results

Parameter	Value
R_1	$3.3 \times 10^{-3} \Omega$
L_1	$6.2 \times 10^{-7} \text{ H}$
M_{12}	$2.0 \times 10^{-9} \text{ H}$
R_2	$3.3 \times 10^{-4} \Omega$
L_2	$3.3 \times 10^{-8} \text{ H}$
M_{21}	$2.0 \times 10^{-9} \text{ H}$

Next, we will calculate the values analytically and compare them with the simulation results. The resistance of the coil can be calculated using the known formula

$$R = \rho \frac{L}{A};$$

$$R_1 = \rho \frac{L_1}{A_1} = 1.667 \times 10^{-8} \cdot \frac{2\pi \cdot 10 \cdot 10^{-3}}{\pi \cdot 10^{-6}} = 3.3 \times 10^{-4} \Omega, \quad (6)$$

$$R_2 = \rho \frac{L_2}{A_2} = 1.667 \times 10^{-8} \cdot \frac{2\pi \cdot 100 \cdot 10^{-3}}{\pi \cdot 10^{-6}} = 3.3 \times 10^{-3} \Omega, \quad (7)$$

results in Eq.(6) and (7) match the calculations from COMSOL listed in Table 3 This confirms the accuracy of COMSOL's computation of coil resistance.

The coil self-inductance can be calculated using the magnetic energy formula

$$W_m = \frac{1}{2} LI^2, \text{ which yields } L = \frac{2}{I^2} \int_{\Omega} W_m d\Omega. \text{ In the simulation of magnetic field}$$

distribution in COMSOL, with the simulated W_m generated from the given current I , we can get:

$$L_1 = \frac{2}{I_1^2} \int_{\Omega} W_1 d\Omega = 6.2 \times 10^{-7} H, \quad (8)$$

$$L_2 = \frac{2}{I_2^2} \int_{\Omega} W_2 d\Omega = 3.3 \times 10^{-8} H. \quad (9)$$

Results in Eq.(8) and Eq.(9) match the calculations from COMSOL listed in Table 3. This confirms the accuracy of COMSOL's computation of coil self-inductance.

The coil mutual inductance can be calculated using the known formula $M = \frac{\pi\mu R_{in}^2}{2R_{out}}$:

$$M = L_{12} = L_{21} = \frac{\pi\mu R_2^2}{2R_1} = 2.0 \times 10^{-9} H. \quad (10)$$

Results in Eq.(10) matches the calculations from COMSOL listed in Table 3, this confirms the accuracy of COMSOL's computation of coil mutual inductance.

Since the coil setup involving the central solenoid coil entails "Coil group", in order to more accurately confirm the accuracy of COMSOL's mutual inductance calculation, we need to benchmark the mutual inductance between the solenoid and single-loop coil computed by COMSOL.

(1) Draw a helical coil with a radius $a = 10$ mm, height $x = 20$ mm, and $N = 10$ turns, and a single-loop coil with a radius $A = 100$ mm. Both coils have a radius of $r_0 = 1$ mm and are made of copper material, as shown in Figure 4-5. Set the "Coil name" of the outer coil to "1" and the "Coil name" of the inner coil to "2".

(2) Set up two "Time-dependent" studies:

(2a) "Study 1" simulates the magnetic field distribution when 1 A of current passes through "Coil 1" and 0 A of current passes through "Coil 2".

(2b) "Study 2" simulates the magnetic field distribution when 0 A of current passes through "Coil 1" and 1 A of current passes through "Coil 2".

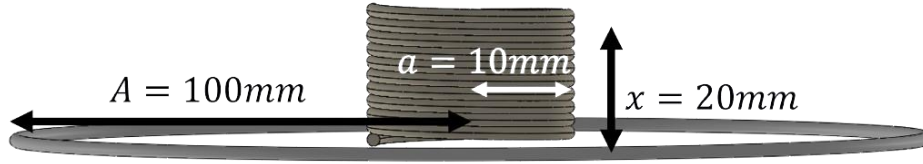


Figure 4-5: Coil Schematic Diagram

The simulation results show that: $M_{12} = 1.941 \times 10^{-8}H$, $M_{21} = 1.941 \times 10^{-8}H$.

The coil mutual inductance can be calculated using the known formula $M = 0.002\pi^2 a \alpha \rho N Q_0$, where Q_0 is obtained from Table 27 in page 115 of "Inductance Calculations: Working Formulas and Tables" by Frederick Grover. Since the calculations in the book are in units of cm, we transfer the units to cm: $a = 1 \text{ cm}$ 、 $x = 1 \text{ cm}$ 、 $A = 10 \text{ cm}$:

$$\begin{aligned} M &= 0.002\pi^2 a \alpha \rho N Q_0 = 0.002\pi^2 \times 1 \times 0.1 \times 0.98 \times 10 \times 1.0035 \\ &= 1.941 \times 10^{-2} \mu H = 1.941 \times 10^{-8} H \end{aligned} \quad (11)$$

where $\alpha = \frac{a}{A} = 0.1$, $\rho = \sqrt{\frac{A^2}{A^2+x^2}} = 0.98$, $N = 10$, $Q_0 = 1.0035$.

Results in Eq.(11) matches the calculations from COMSOL. This confirms the accuracy of COMSOL's computation of mutual inductance when the single-loop coil is placed at the bottom of the helical coil. However, we still need to compute the accuracy of COMSOL's mutual inductance calculation when the single-loop coil is placed in the middle of the helical coil.

In Figure 4-6 (b), the circuit diagram represents the scenario where the single-loop coil is placed at the bottom of the helical coil. For simplicity, coil resistances are omitted. In the diagram, L represents the coil self-inductance, M represents the mutual inductance between the two coils, I represents the current flowing through the coils, and $V = M_{12} \frac{dI_1}{dt}$.

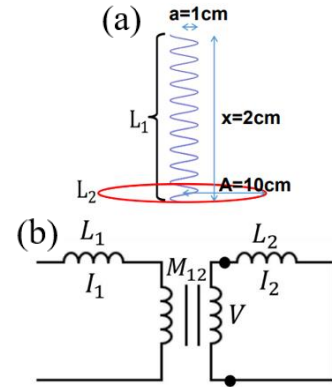


Figure 4-6 (a): Coil Diagram
(b): Circuit Diagram

When we place the single-loop coil in the middle of the helical coil, it can be considered as placing the single-loop coil between two identical helical coils, as shown in Figure 4-7 (a). In this case, the two identical helical coils can be viewed as being connected in series. Therefore, in Figure 4-7(b), we have $V = M_{12} \frac{dI_1}{dt} + M_{32} \frac{dI_3}{dt} = (M_{12} + M_{32}) \frac{dI}{dt} = M \frac{dI}{dt}$, indicating that M should be the sum of the mutual inductances between the two identical helical coils and the single-loop coil.

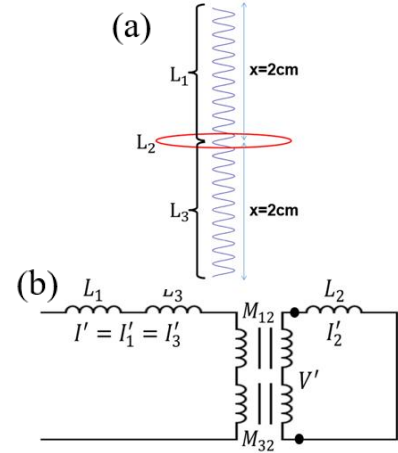


Figure 4-7 (a): Coil Diagram
(b): Circuit Diagram

The coil mutual inductance can be calculated using the known formula $M = 0.002\pi^2 a \alpha \rho N Q_0$. By having L , equals to L_3 , we have:

$$\begin{aligned} M_{32} = M_{12} &= 0.002\pi^2 a \alpha \rho N Q_0 = 0.002\pi^2 \times 1 \times 0.1 \times 0.98 \times 10 \times 1.0035 \\ &= 1.941 \times 10^{-2} \mu H = 1.941 \times 10^{-8} H, \end{aligned} \quad (12)$$

$$M' = M_{32} + M_{12} = 3.882 \times 10^{-8} H, \quad (13)$$

where $\alpha = \frac{a}{A} = 0.1$, $\rho = \sqrt{\frac{A^2}{A^2 + x^2}} = 0.98$, $N = 10$, $Q_0 = 1.0035$.

To simulate in COMSOL, please follow the following procedures:

- (1) Draw a helical coil with a radius $a = 10$ mm, height $x = 40$ mm, and $N = 20$ turns, and a single-loop coil with a radius $A = 100$ mm in COMSOL. Both

coils have a radius of $r_0 = 1 \text{ mm}$ and are made of copper material, as shown in Figure 3-8. Set the "Coil name" of the outer coil to "1" and the "Coil name" of the inner coil to "2".

(2) Set up two "Time-dependent" studies:

(2a) "Study 1" simulates the magnetic field distribution when 1 A of current passes through "Coil 1" and 0 A of current passes through "Coil 2".

(2b) "Study 2" simulates the magnetic field distribution when 0 A of current passes through "Coil 1" and 1 A of current passes through "Coil 2".

The simulation results show that $mf.L_{2,1} = 3.882 \times 10^{-8}H$, $mf.L_{1,2} = 3.882 \times 10^{-8}H$. The results match the calculations in Eq.(13). We can confirm the accuracy of COMSOL's computation of mutual inductance between the helical coil and surrounding coils.

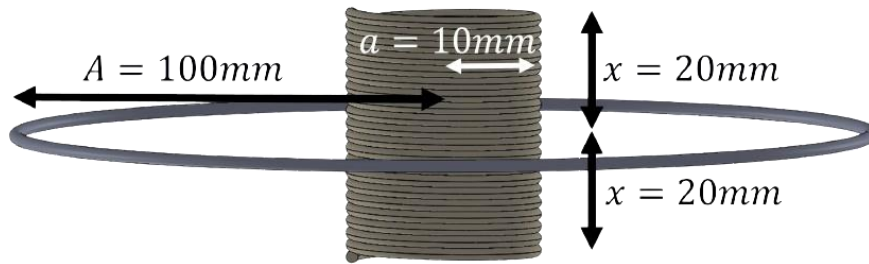


Figure 4-8: Coil Schematic Diagram

4.4. Calculation of the eddy current using the full circuit equation

We can calculate the induced current on inner vacuum vessel wall generated by the time-varying current in central solenoid using the full circuit equation:

$$V = M \frac{dI}{dt} + RI. \quad (14)$$

It states that the total voltage “ V ” in a closed loop equals its induced voltage “ $M \frac{dI}{dt}$,” plus the voltage drop due to resistance “ RI ”. Here, V represents voltage, I represents current, M represents inductance, and R represents resistance.

For convenience in calculations, we have V and I in the vector form to represent

voltages and currents in all coils and ring elements of inner vacuum vessel components. On the other hand, M and R are written in the matrix form including the self-inductance and the resistance of each coil and ring elements of the inner vacuum vessel wall, and the mutual inductance between each coil and ring elements of the inner vacuum vessel wall. In addition, subscript c represents coils in the Tokamak device, such as the central solenoid, PFC, TFC, etc.; subscript v represents components in the Tokamak device's vacuum vessel; subscript p represents the plasma. Therefore, \vec{I}_{cvp} is a column vector of size $n + 1$, representing the currents of the total n components of coils and vacuum vessel components in the Tokamak device plus the plasma current. \vec{v}_{cvp} is also a column vector of size $n + 1$, representing the external voltages applied to the total n components of coils and vacuum vessel components in the Tokamak device plus the loop voltage of plasma. \vec{R}_{cvp} is a diagonal matrix of size $(n + 1) \times (n + 1)$, representing the electrical resistance of the total n components of coils and vacuum vessel components in the Tokamak device plus the plasma circuit. \vec{M}_{cvp} is a symmetric matrix of size $(n + 1) \times (n + 1)$, representing the self-inductance (diagonal elements) and mutual inductance (off-diagonal elements) of the total n components of coils and vacuum vessel components in the Tokamak device plus the plasma. Therefore, Eq.(14) can be written explicitly as

$$\begin{aligned}
\vec{V} &= \vec{M} \frac{d\vec{I}}{dt} + \vec{R}\vec{I} \\
\Rightarrow \begin{bmatrix} V_{c1} \\ V_{c2} \\ \vdots \\ V_{v1} \\ V_{v2} \\ \vdots \\ V_p \end{bmatrix} &= \begin{bmatrix} L_{c1} & M_{c1,c2} & M_{c1,c3} & \cdots & M_{c1,v1} & M_{c1,v2} & M_{c1,v3} & \cdots & M_{c1,p} \\ M_{c2,c1} & L_{c2} & M_{c2,c3} & \cdots & M_{c2,v1} & M_{c2,v2} & M_{c2,v3} & \cdots & M_{c2,p} \\ M_{c3,c1} & M_{c3,c2} & L_{c3} & \cdots & M_{c3,v1} & M_{c3,v2} & M_{c3,v3} & \cdots & M_{c3,p} \\ \vdots & \vdots & \vdots & \vdots & \vdots & \vdots & \vdots & \vdots & \vdots \\ M_{v1,c1} & M_{v1,c2} & M_{v1,c3} & \cdots & L_{v1} & M_{v1,v2} & M_{v1,v3} & \cdots & M_{v1,p} \\ M_{v2,c1} & M_{v2,c2} & M_{v2,c3} & \cdots & M_{v2,v1} & L_{v2} & M_{v2,v3} & \cdots & M_{v2,p} \\ M_{c3,c1} & M_{v3,c2} & M_{v3,c3} & \cdots & M_{v3,v1} & M_{v3,v2} & L_{v3} & \cdots & M_{v3,p} \\ \vdots & \vdots & \vdots & \vdots & \vdots & \vdots & \vdots & \vdots & \vdots \\ M_{p,c1} & M_{p,c2} & M_{p,c3} & \cdots & M_{p,v1} & M_{p,v2} & M_{p,v3} & \cdots & L_p \end{bmatrix} \begin{bmatrix} \dot{I}_{c1} \\ \dot{I}_{c2} \\ \vdots \\ \dot{I}_{v1} \\ \dot{I}_{v2} \\ \vdots \\ \dot{I}_p \end{bmatrix} \\
&+ \begin{bmatrix} R_{c1} & 0 & \cdots & 0 & 0 & \cdots & 0 \\ 0 & R_{c2} & \cdots & 0 & 0 & \cdots & 0 \\ \vdots & \vdots & \vdots & \vdots & \vdots & \vdots & \vdots \\ 0 & 0 & \cdots & R_{v1} & 0 & \cdots & 0 \\ 0 & 0 & \cdots & 0 & R_{v2} & \cdots & 0 \\ \vdots & \vdots & \vdots & \vdots & \vdots & \vdots & \vdots \\ 0 & 0 & \cdots & 0 & 0 & \cdots & R_p \end{bmatrix} \begin{bmatrix} I_{c1} \\ I_{c2} \\ \vdots \\ I_{v1} \\ I_{v2} \\ \vdots \\ I_p \end{bmatrix}. \tag{15}
\end{aligned}$$

Eq.(14) can be solved numerically using finite difference method:

$$\begin{aligned}
\vec{V} &= \vec{M} \frac{d\vec{I}}{dt} + \vec{R}\vec{I} \Rightarrow \vec{V} = \vec{M} \frac{\vec{I}' - \vec{I}}{\Delta t} + \vec{R}\vec{I} \Rightarrow \vec{V} = \vec{M} \frac{\vec{I}'}{\Delta t} + \vec{M} \frac{\vec{I}}{\Delta t} + \vec{R}\vec{I} \\
&= \vec{M} \frac{\vec{I}'}{\Delta t} + \left(\frac{\vec{M}}{\Delta t} + \vec{R} \right) \vec{I} \Rightarrow \vec{I}' \frac{\vec{M}}{\Delta t} = \vec{V} + \left(\frac{\vec{M}}{\Delta t} + \vec{R} \right) \vec{I} \\
\Rightarrow \vec{I}' &= \left(\frac{\vec{M}}{\Delta t} \right)^{-1} \left[\vec{V} + \left(\frac{\vec{M}}{\Delta t} + \vec{R} \right) \vec{I} \right]. \tag{16}
\end{aligned}$$

Notice that matrix \vec{M} and \vec{R} are constants. By proving $\vec{v}(t)$, we can obtain $\vec{I}(t)$ at any time.

Taking the example of calculating the induced current on inner vacuum vessel wall due to the time-varying current in central solenoid, let's provide the time-varying voltage V_{c1} for central solenoid, as shown in Figure 4-9(a). Inner vacuum vessel wall does not have an external power source, so its voltage V_{v1} remains constantly zero:

$$\vec{V}_{cvp} = \begin{bmatrix} V_{c1} \\ V_{c2} \\ \vdots \\ V_{v1} \\ V_{v2} \\ \vdots \\ V_p \end{bmatrix} = \begin{bmatrix} V_{cs} \\ 0 \\ 0 \\ \vdots \\ 0 \end{bmatrix}. \quad (17)$$

With M and R in Eq.(18) and Eq.(19) calculated from COMSOL. We can calculate the induced current on the vacuum vessel wall as illustrated in Figure 4-9(b).

$$M = \begin{bmatrix} 2.1E-03 & 8.87E-06 & 1.03E-05 & 1.03E-05 & 8.71E-06 \\ 8.87E-06 & 1.67E-07 & 2.54E-08 & 2.29E-09 & 6.17E-10 \\ 1.03E-05 & 2.54E-08 & 1.67E-07 & 2.53E-08 & 2.31E-09 \\ 1.03E-05 & 2.29E-09 & 2.53E-08 & 1.67E-07 & 2.53E-08 \\ 8.71E-06 & 6.17E-10 & 2.31E-09 & 2.53E-08 & 1.67E-07 \end{bmatrix}, \quad (18)$$

$$R = \begin{bmatrix} 2.9E-02 & 0 & 0 & 0 & 0 \\ 0 & 4.25E-04 & 0 & 0 & 0 \\ 0 & 0 & 4.25E-04 & 0 & 0 \\ 0 & 0 & 0 & 4.25E-04 & 0 \\ 0 & 0 & 0 & 0 & 4.25E-04 \end{bmatrix}. \quad (19)$$

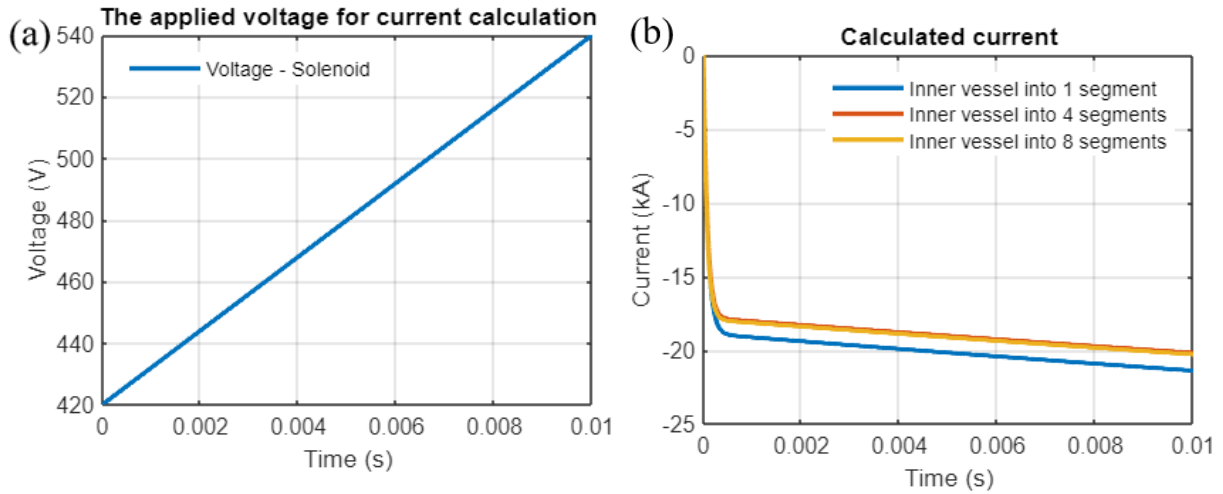


Figure 4-9 (a): Time-varying voltage across the central solenoid
(b): Induced current on the vacuum vessel wall

To confirm the accuracy of the calculations, we divided the vacuum vessel wall into one, four, and eight equal segments, as shown in Figure 4-10. It can be observed in Figure 4-9 (b) that as we increase the number of segments, the solutions for the induced current converge. This convergence occurs because finer segmentation of the inner wall allows for better modeling of the mutual inductance between components.

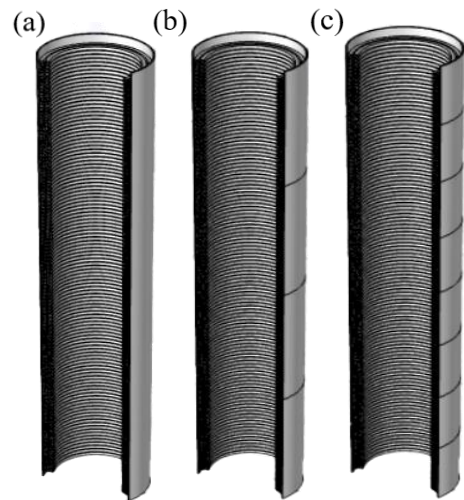


Figure 4-10 (a): One division
(b): Four division
(c): Eight division

4.5. Discussion

Through the calculations, we have confirmed the ability to compute induced currents using the full circuit equation. In the future, we will incorporate all coils and vessel components inside the Tokamak device into our calculations. By calculating all induced currents generated within the Tokamak, we can refine our design and obtain more accurate data. This method can also be applied to calculate the required current variations in the central solenoid for reaching breakdown voltage to form a plasma, and providing the plasma current at our desired peak value after plasma generation.

5. Future work

In the first half of 2024, I will focus on establishing a program system that can calculate self-inductance and mutual inductance between coils based on provided coil positions and specifications. Then, I will be able to use the full circuit equation to compute the induced currents generated. Additionally, I will utilize COMSOL to simulate the magnetic field distribution inside the Tokamak device, enabling the calculation of coil designs necessary to achieve the desired magnetic field in the upward Z direction (B_z) at the center of the vacuum chamber. In the second half of the year, I will begin the construction of a small-scale Tokamak device for testing components and laboratory teaching purposes based on the accumulated data obtained from the calculations conducted so far.

6. Conclusion

In 2023, my main accomplishments were related to the design calculations of the Tokamak device. I utilized COMSOL to simulate the ohmic heating and cooling requirements of the coils inside the Tokamak device and verified the accuracy of the COMSOL simulations through benchmark calculations. The results indicated that cooling systems would not be necessary for the subsequent design of the Tokamak device. Additionally, I used COMSOL to compute the resistance and inductance required for calculating induced currents and confirmed the accuracy of these calculations through benchmarking. Furthermore, I confirmed the feasibility of using the full circuit equation to compute the induced currents generated on inner vacuum vessel wall due to the time-varying current in central solenoid. Through this method, we can calculate the induced currents generated between other components within the Tokamak device, allowing us to consider their effects in subsequent designs. Moving forward, we will also utilize this method to compute the breakdown voltage required

for forming a plasma and to determine the current variations needed in the central solenoid to maintain the plasma current in an ideal state.

Reference

[1] Hyun-Tae Kim et al. Development of full electromagnetic plasma burn-through model and validation in MAST. Nucl. Fusion 62, 126012, 2022.

[2] Po-Yu Chang. 國科會磁約束高溫電漿計畫-子計畫一執行情形.

[3] Frederick W. Grover. (2004). Inductance Calculations: Working Formulas and Tables. Dover Publications.